Neuron, Vol. 39, 375–386, July 17, 2003, Copyright ©2003 by Cell Press

The Nose Smells What the Eye Sees: Crossmodal Visual Facilitation of Human Olfactory Perception

Jay A. Gottfried* and Raymond J. Dolan
Functional Imaging Laboratory
Wellcome Department of Imaging Neuroscience
12 Queen Square
London WC1N 3BG
United Kingdom

Summary

Human olfactory perception is notoriously unreliable, but shows substantial benefits from visual cues, suggesting important crossmodal integration between these primary sensory modalities. We used event-related fMRI to determine the underlying neural mechanisms of olfactory-visual integration in the human brain. Subjects participated in an olfactory detection task, whereby odors and pictures were delivered separately or together. By manipulating the degree of semantic correspondence between odor-picture pairs, we show a perceptual olfactory facilitation for semantically congruent (versus incongruent) trials. This behavioral advantage was associated with enhanced neural activity in anterior hippocampus and rostromedial orbitofrontal cortex. We suggest these findings can be interpreted as indicating that human hippocampus mediates reactivation of crossmodal semantic associations, even in the absence of explicit memory processing.

Introduction

In a recent wine-tasting study conducted at the University of Bordeaux, 54 enology students provided odor descriptions of red and white wines (Morrot et al., 2001). Prior to the experiment, and without the subjects' knowledge, a white wine was surreptitiously colored with odorless red dye. As a result, subjects consistently described the "red" white wine using language typically reserved for red wine and avoided the use of white wine terms. Thus, in the absence of appropriate visual information, wine odor had minimal impact on olfactory discrimination, and despite "expertise" among subjects, the visual contextual cue dominated.

If nothing else, this report underscores a certain ambiguity in human olfactory discrimination, even among professionals. Psychological research has shown that identification of single odors is poor, but improves when relevant semantic (e.g., verbal) information is available (Cain, 1979). Basic aspects of olfactory processing, including detection thresholds, adaptation rates, and intensity judgments are also strongly modulated by visual, perceptual, and cognitive factors (Zellner and Kautz, 1990; Dalton, 1996; Dalton et al., 2000; Distel and Hudson, 2001). In turn, odor semantics have been shown to modulate human event-related potentials evoked by verbal (Lorig et al., 1993) or visual (Grigor et al., 1999; Sarfarazi et al., 1999) stimuli. These examples suggest that interactions between olfactory and other sensory modalities may contribute to effective odor perception, and these interactions could be sustained via multimodal convergence.

How olfactory-visual integration, the focus of the present study, is mediated in the human brain is not understood. Animal studies indicate that various anatomical sites receive converging input from both sensory modalities. One potential site is the hippocampus, a structure that can be accessed directly or indirectly by all sensory modalities (Deadwyler et al., 1987; Small, 2002). Such an anatomical arrangement potentially allows it to recruit multiple sensory features in the service of mnemonic functions (Wood et al., 1999; Save et al., 2000). With respect to olfaction, the hippocampus is separated by as few as three synapses from odor receptor neurons in the nasal mucosa, projecting via the olfactory bulb and the entorhinal cortex (Schwerdtfeger et al., 1990), and odor-specific waves of rhythmic activity have been documented in rodent dentate gyrus (Chapman et al., 1998; Vanderwolf, 2001). Interestingly, human lesion studies have shown that postsurgical epilepsy patients with damage to hippocampus and adjacent medial temporal structures are profoundly impaired on a variety of crossmodal odor tasks, despite preservation of elementary olfactory function (Eichenbaum et al., 1983; Eskenazi et al., 1983). However, such data are always tempered by the possibility that remote (extratemporal) neocortical changes could otherwise explain the behavioral deficits in this patient group. Regarding the visual domain, the hippocampus has ready access to visual information by way of perirhinal and parahippocampal cortices (Suzuki and Amaral, 1994), and recent findings suggest a direct monosynaptic route from visual association cortex to area CA1 of primate hippocampus (Rockland and Van Hoesen, 1999). Human hippocampal neurons have also been found in single-unit recordings that respond selectively to different categories of visual stimuli (Kreiman et al., 2000).

Another site that may participate in multimodal integration is the orbitofrontal cortex (OFC). In nonhuman primates, this region has been shown to receive afferent input from both primary olfactory (piriform) cortex and visual association areas (Carmichael and Price, 1995), and individual OFC neurons have been identified in single-unit recordings that respond to olfactory and visual stimulation either separately or in combination (Rolls and Baylis, 1994). It has been suggested that such a confluence of sensory streams in OFC could help subserve higher-order control of flavor perception and feeding behavior (Carmichael and Price, 1995). In human neuroimaging experiments of olfaction, OFC is among the most consistently activated structures (Zatorre et al., 1992; Zald and Pardo, 1997; Sobel et al., 2000), and a recent fMRI study of olfactory-visual associative learning highlighted its participation in the establishment of crossmodal associations between these two stimulus modalities (Gottfried et al., 2002b).

Finally, it is unclear whether other polysensory areas,

*Correspondence: j.gottfried@fil.ion.ucl.ac.uk

such as intraparietal sulcus (IPS) and superior temporal sulcus (STS), mediate olfactory-visual integration. These regions are typically associated with multimodal interactions between visual, auditory, and somatosensory stimuli (Bruce et al., 1981; Hikosaka et al., 1988; Andersen, 1997; Duhamel et al., 1998), but a place for olfactory cues has not been elucidated. While direct inputs from piriform cortex to IPS or STS remain unidentified, olfactory projections through areas of OFC and amygdala, which are themselves coupled to IPS and STS (Jones and Powell, 1970; Mizuno et al., 1982; Amaral and Price, 1984; Iwai and Yukie, 1987; Cavada and Goldman-Rakic, 1989; Morecraft et al., 1993; Carmichael and Price, 1995), could represent indirect routes for the transmission of olfactory information. In this regard, recent neuroimaging and magnetoencephalographic studies of human olfaction, using a variety of different paradigms, elicit activations in STS and parietal cortex (Kettenmann et al., 1996; Savic et al., 2000; Zatorre et al., 2000; Dade et al., 2001; Poellinger et al., 2001).

Human imaging studies of multisensory integration have chiefly focused on audio-visual (Calvert et al., 2000) and visuo-tactile (Macaluso et al., 2000) combinations. Among the chemical senses, there have been relatively few investigations. One fMRI study of gustatory and lingual somatosensory interactions revealed significant effects in portions of opercular cortex (Cerf-Ducastel et al., 2001). In a PET study of flavor processing, Small et al. (1997) delivered blocks of olfactory and gustatory inputs separately or together (matched or mismatched) and demonstrated significant deactivations in areas including visual cortex, precuneus, basal forebrain, OFC, and insula.

Here, we combined event-related fMRI techniques with an olfactory detection task (Figure 1) to characterize olfactory-visual integration in the human brain. Odors and pictures were presented either independently (unimodal) or in combination (bimodal). During bimodal conditions, the odor-picture pairs could be either semantically related or unrelated. Our paradigm conformed to a modified factorial design and enabled us to explore two different aspects of crossmodal processing. First, we tested the formal interaction of odors and pictures to highlight bimodal responses exceeding the mere sum of unimodal responses. This approach identified brain regions showing bimodal response enhancement, a general property of multisensory neurons (Stein and Meredith, 1993) that has been recently demonstrated in fMRI studies of audio-visual integration (Calvert et al., 2000). Second, the manipulation of semantic correspondence between odor-picture pairs allowed us to identify mechanisms mediating visual semantic modulation of olfactory perception. On the basis of the anatomical and behavioral considerations outlined above, we hypothesized that regions of OFC and hippocampus would participate in crossmodal processing and exhibit sensitivity to semantic variations between odors and pictures.

Results

Behavioral Data

Congruency Ratings

In post hoc ratings of perceived semantic congruency between odor-picture pairs (0 to +10), subjects reported the "congruent" items were more semantically alike than the "incongruent" pairs (Figure 2A). Congruency ratings were: *pleasant* congruent, 7.1 $\pm$ 0.29; *unpleasant* congruent, 6.15 $\pm$ 0.38; *pleasant* incongruent, 0.85 $\pm$ 0.23; and *unpleasant* incongruent, 1.09 $\pm$ 0.24 (mean $\pm$ SEM). There was a significant difference among these scores ($\chi^2 = 39.2$; df = 3; $p < 0.001$; Friedman test), and in post hoc comparisons, the congruent stimuli received significantly higher ratings than the incongruent stimuli ($p < 0.01$; Wilcoxon Test).

Odor Detection

Olfactory perception was facilitated in the presence of semantically congruent (versus incongruent) pictures. Analysis of reaction times (RTs) shows that subjects detected the odors significantly more quickly in the bimodal congruent (1427 $\pm$ 82 s), compared to both bimodal incongruent (1502 $\pm$ 98 s) and unimodal olfactory (1539 $\pm$ 95 s), conditions (mean $\pm$ SEM) (Figure 2B). Repeated measures ANOVA revealed a significant main effect of condition ($F_{1.4,19} = 9.822$; $p < 0.01$; Greenhouse-Geisser corrected), and in post hoc t tests, the RT difference between OV-c and OV-i was significant ($p < 0.05$; two-tailed). There was also a significant difference between OV-c and O ($p < 0.05$), but the comparison between OV-i and O was not significant ($p = 0.16$). Responses were also significantly more accurate for semantically congruent (93.5% $\pm$ 1.9%) than incongruent (88.3% $\pm$ 1.6%) conditions (Figure 2C), when based on subjects' judgments of odor presence (yes/no). There was a significant main effect of condition (repeated-measures ANOVA; $F_{4,56} = 6.737$; $p < 0.05$), and post hoc tests confirmed that the accuracy differences between OV-c and OV-i were significant ($p < 0.05$).

Because each picture item was repeated three times (once each in V, OV-c, and OV-i conditions), it is possible that item sequence could account for the congruency-specific response gains. For example, if the first presentation of a given picture occurred in the unimodal V condition (eliciting a "no odor" response), subjects could have learned that subsequent presentations of that picture (either as OV-c or OV-i) would necessitate a "yes odor" response, leading to behavioral enhancement irrespective of semantic congruency effects. To rule this out, the picture-specific RTs for each OV-c trial were divided into events occurring either before or after its appearance in the unimodal V condition, collapsed across subjects. We then tested for differences in post-V bimodal versus pre-V bimodal responses but failed to show any effect of item sequence ($p = 0.30$; two-tailed paired t test). Moreover, by comparing subject-specific RTs (for the OV-c condition) between the first and second halves of the experiment, we discounted the possibility that bimodal congruent responses were significantly faster in later parts of the study ($p = 0.17$).

Respiratory Measurements

Subject-specific sniff peak amplitudes were averaged over each condition and normalized to the baseline to permit group analysis. There was a significant main effect of condition ($F_{4,52} = 14.879$; $p < 0.01$; repeated measures ANOVA), and pairwise t tests revealed that sniff amplitudes were significantly larger by 7%–11% in the odor-absent conditions (V and Bas.) compared to the odor-present conditions (O, OV-c, and OV-i) (all $p <$ 0.01). This finding is compatible with the idea that sub-

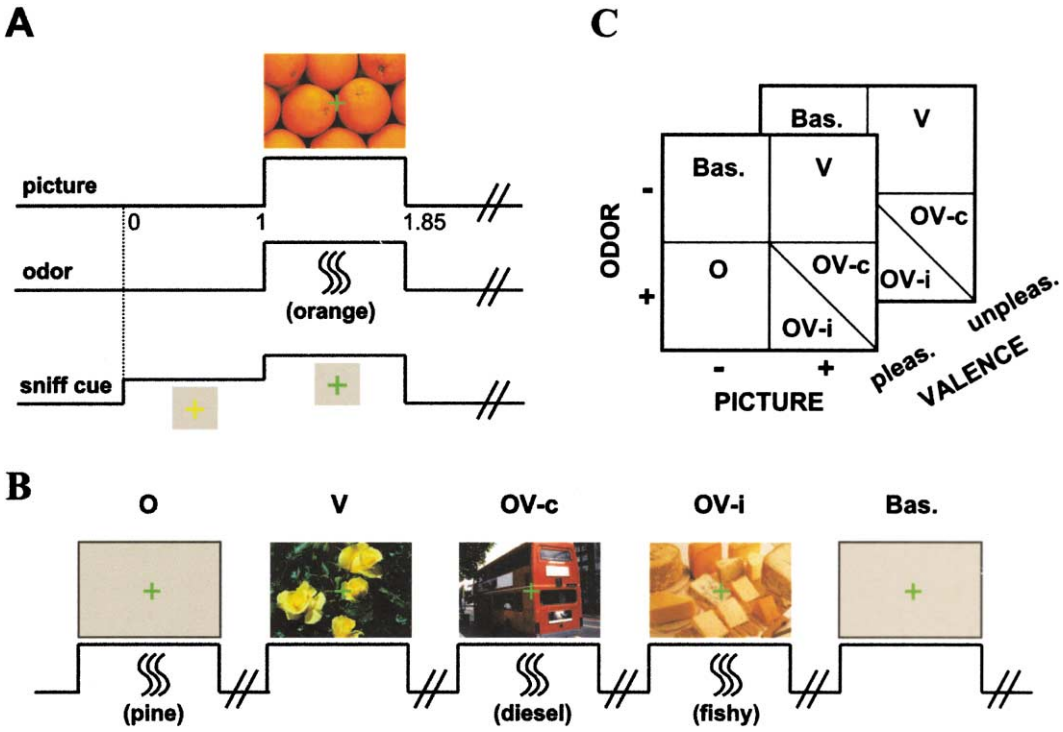

Figure 1. Experimental Task and Paradigm

(A) In this example of a bimodal congruent trial, a 1 s preparatory cue (yellow cross-hair) heralded the simultaneous delivery of a matching picture and odor. Subjects sniffed for the 850 ms duration of the sniff cue (green cross-hair), which overlapped stimulus presentation, then indicated as quickly and as accurately as possible whether an odor was present ("yes") or absent ("no").

(B) The five different condition types included unimodal olfactory (O), unimodal visual (V), bimodal congruent (OV-c), bimodal incongruent (OV-i), and a low-level baseline without odor or picture (Bas.).

(C) The experiment conformed to a 2 × 2 × 2 modified factorial design (odor × picture × valence), in which bimodal conditions were assorted into semantically congruent and incongruent conditions.

jects sniffed more deeply in the absence of odor, in order to be certain that odor had not been delivered. However, there were no significant differences between odor-absent conditions, nor between odor-present conditions. Importantly, for the two critical imaging analyses (odor × picture interaction, and congruent-incongruent), there were no significant differences in either sniff peak amplitude ($p > 0.19$) or sniff latency (time-to-peak) ($p > 0.12$).

Neuroimaging Data

Olfactory Stimulation

We first evaluated the main effect of olfaction (i.e., [O + OV] − [V + Bas.]), collapsed across congruency. This contrast highlights regions preferentially sensitive to olfactory stimulation. Note that the inclusion of the low-level baseline condition (Bas.) ensures an appropriately balanced contrast. Significant activation was identified in right posterior piriform cortex (*x*, *y*, *z* coordinates: 27, 3, −27; $Z = 5.19$; $p < 0.05$, corrected for whole-brain volume) (Figure 3A), which extended into peri-insular cortex anteriorly and amygdala and entorhinal cortex posteriorly. Temporal piriform activation on the left (−27, 6, −33; $Z = 3.40$; $p < 0.05$, corrected for small-volume [SVC]) was contiguous with periamygdaloid cortex. Odor-specific responses were also detected in bilateral centroposterior OFC and left amygdala (Table 1; Figures 3B and 3C), each of which closely overlapped areas identified in prior studies of human olfactory processing (Zald and Pardo, 1997; Sobel et al., 2000; Royet et al., 2000; Gottfried et al., 2002a).

In addition, valence effects were examined. A two-way interaction of olfaction × valence, effectively comparing the main effects of unpleasant and pleasant olfaction, revealed significant activity in left anterior piriform cortex (Table 1). This response reflected greater differential activation by the "unpleasant" O and OV conditions in a region adjacent to anterior piriform regions previously associated with unpleasant odor valence (Gottfried et al., 2002a), lending further support to the idea of functional heterogeneity within human piriform cortex. Finally, in the simple effect of unimodal *pleasant* odor (pleasant O − Bas.), activations were identified in right medial OFC (18, 27, −15; $Z = 3.98$; $p < 0.05$ SVC), which has been described in other imaging studies of pleasant odor (Gottfried et al., 2002a; Anderson et al., 2003), though OFC responses were not detected in a similar contrast of the *unpleasant* odor. In this latter circumstance, with only 16 presentations of each condition, it is possible that there was insufficient statistical power to detect differential simple effects of odor valence.

Multisensory Olfactory-Visual Interactions

We next examined for regions preferentially responsive to a combination of olfactory-visual input. The crossmo-

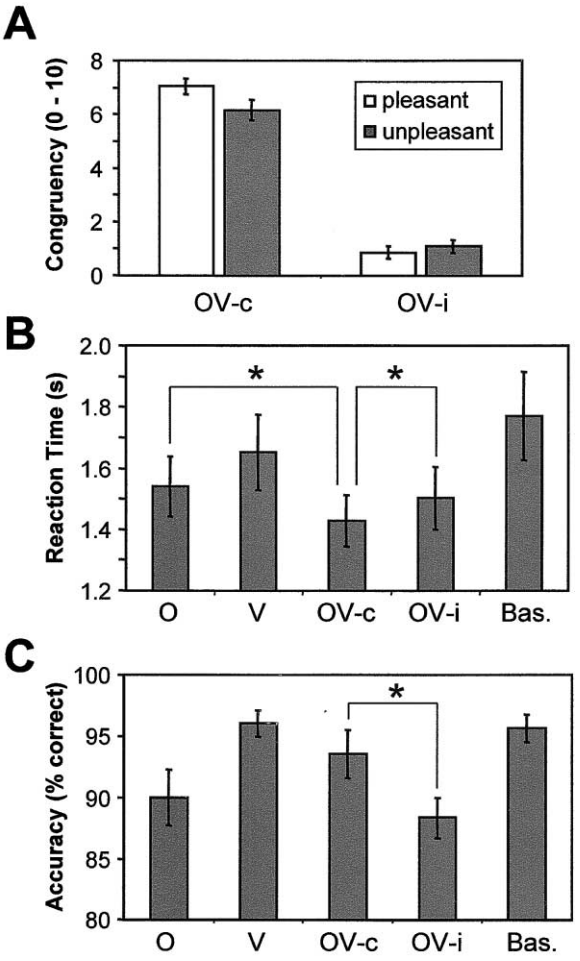

Figure 2. Behavioral Results

(A) Subjects rated the bimodal congruent stimuli to be more semantically alike than odor-matched incongruent stimuli (means ± SEM), for each valence level.

(B) Mean reaction times (±SEM) were significantly faster when odors appeared with semantically congruent pictures (OV-c), in comparison to semantically incongruent pictures (OV-i), or when presented alone (O); *$p < 0.05$ (two-tailed paired t test).

(C) Mean response accuracy was significantly higher in the congruent, compared to the incongruent, condition; *$p < 0.05$.

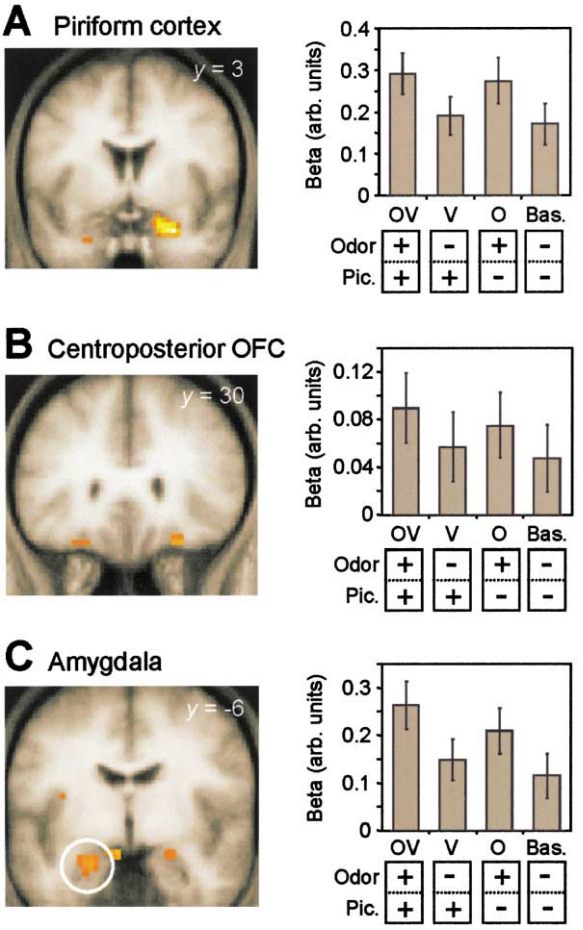

Figure 3. Brain Activations Evoked by Olfactory Stimulation

The main effect of olfaction was associated with significant neural activity in (A) primary olfactory (piriform) cortex ($x = 21$, $y = -3$, $z = -24$), (B) centroposterior OFC (−21, 30, −21), and (C) amygdala (−21, −6, −24). The SPMs are superimposed on coronal sections of the averaged, normalized T1-weighted scan (n = 15 subjects) and thresholded at $p < 0.001$. In this and all subsequent figures, the right side of the images corresponds to the right side of the brain ("neurological" convention). The condition-specific parameter estimates (betas) from these regions were averaged across subjects and shown in adjacent plots, illustrating greater activation in odor-present (OV and O) than in odor-absent (V and Bas.) conditions (means ± SEM).

dal interaction of olfaction × vision, or [OV − Bas.] − ([O − Bas.] + [V − Bas.]), was used to identify bimodal activity exceeding the sum of unimodal responses. Response enhancements of this sort have previously been described in animal (Stein and Meredith, 1993) and human (Calvert et al., 2000) studies of multisensory integration involving nonolfactory stimuli. In this contrast, significant enhanced activity was observed in left rostromedial OFC (−15, 39, −15; $Z = 3.18$; $p = 0.059$ SVC). Parameter estimate plots established that the interaction reflected greater differential responses to bimodal OV compared to the unimodal O plus V conditions, when adjusted for the common baseline (Bas.) activity (Figure 4A). Enhanced responses were also observed in the depths of the posterior IPS, just medial to the transverse occipital sulcus (Figure 4B). Here, the parameter estimates show that posterior IPS is a visually responsive region (evident in the main effect of vision, $p < 0.001$) as well as an area sensitive to combined olfactory-visual presentations, with responses to OV being augmented over and above those seen in a simple addition of O and V (baseline adjusted). Additional activations were seen in STS and posterior cingulate cortex (Table 2).

Note that by collapsing across congruency, we made no assumptions that the odor × picture interaction necessarily depended on semantic features, but simply on temporal synchrony of their presentation. Indeed, in many animal studies of crossmodal integration, it is spatial or temporal correspondence that dictates multisensory response enhancement, not semantic attributes (Stein and Meredith, 1993). There are also examples in the human neuroimaging literature indicating that temporal factors are critical to crossmodal processing

Table 1. Regions Activated by Olfactory Stimulation

Brain Region	MNI Coordinates (mm) x	y	z	Peak *Z*	p value
Main effect of olfaction					
Right piriform cortex	27	3	−27	5.19	$p < 0.05$[a]
Left piriform cortex	−27	6	−33	3.40	$p < 0.05$[b]
Right centroposterior OFC	30	36	−15	3.96	$p < 0.05$[b]
	27	33	−21	3.89	$p < 0.05$[b]
Left centroposterior OFC	−30	36	−18	3.68	$p < 0.05$[b]
	−21	30	−21	3.27	$p < 0.05$[b]
Left amygdala	−21	−6	−24	3.60	$p < 0.05$[b]
Left insula	−36	−3	15	3.55	$p < 0.001$
	−39	6	−15	3.20	$p < 0.001$
Right insula	36	9	−21	3.43	$p < 0.001$
Left anterior cingulate cortex	−9	21	45	3.45	$p < 0.001$
Two-way interaction of olfaction × valence (unpleasant > pleasant)					
Left anterior piriform cortex	−18	9	−21	3.47	$p < 0.001$

[a] Corrected for whole-brain volume.
[b] Corrected for multiple comparisons across a small volume of interest.

(Bushara et al., 2001; Calvert et al., 2001). Nevertheless, in our study it is possible that integration might occur to a greater extent for the bimodal congruent condition. Consequently, we reexamined the odor × picture interaction by exchanging OV-c for OV. Compared to the above (collapsed) interaction, this analysis revealed a very similar pattern of activations in rostromedial OFC (−15, 39, −15; $Z = 3.42$; $p < 0.05$ SVC), posterior IPS (−36, −78, 18; $Z = 3.82$; and −24, −81, 21; $Z = 3.30$; $p < 0.001$ uncorrected), and STS (66, −42, 6; $Z = 3.33$; $p < 0.001$ uncorrected) (Table 2). In contrast, by substituting the bimodal incongruent (OV-i) condition into the interaction, neural activity was also detected in IPS (−24, −81, 21; $Z = 3.42$; $p < 0.001$ uncorrected), as well as in posterior cingulate cortex (−9, −24, 36; $Z = 3.62$; $p < 0.001$ uncorrected), but not in OFC (at a liberal threshold of $p < 0.01$). These results demonstrate that the odor × picture interaction in OFC is driven more by semantically congruent items, a finding in accord with an analysis directly comparing OV-c to OV-i (see below). On the other hand, both congruent and incongruent interactions activated IPS, suggesting this region is relatively insensitive to semantic effects.

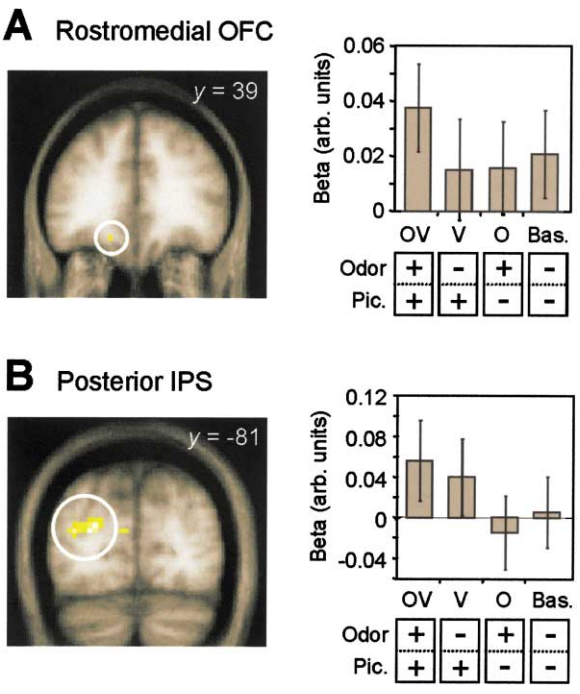

Figure 4. Brain Activations Evoked by the Interaction of Odors and Pictures

(A) Significant activity was observed in left rostromedial OFC (−15, 39, −15). The SPM is superimposed on the averaged T1-weighted coronal scan (threshold, $p < 0.001$). Plots of the parameter estimates show that bimodal responses to OV are higher than the unimodal sum of O + V, when adjusted for the common baseline (Bas.) activity. (B) The interaction also highlighted responses in posterior IPS (−27, −81, 18). The corresponding parameter estimates are representative of multisensory response enhancement, which partially reflects nonsignificant response deactivation to the unimodal olfactory condition.

Crossmodal Semantic Congruency

The behavioral results showed that olfactory detection was facilitated in the presence of semantically related (versus unrelated) visual cues. A key objective of the experiment was to determine the underlying mechanisms of this crossmodal facilitation by comparing bimodal congruent and incongruent conditions. The contrast [OV-c] – [OV-i] identified significant activation in left anterior hippocampus (−27, −12, −24; $Z = 4.26$; $p < 0.05$ SVC) (Table 3; Figure 5A). Activity in right anterior hippocampus was evident at reduced threshold (21, −12, −21; $Z = 2.56$; $p = 0.005$ uncorrected). Significant congruency-evoked responses were also observed in left rostromedial OFC (−3, 39, −18; $Z = 3.72$; −12, 42, −18; $Z = 3.60$; both $p < 0.05$ SVC) (Figure 5B). These peak responses were not modulated by valence, even when evaluated at a lower threshold ($p < 0.05$ uncorrected). We note that the activations were discretely localized to orbitofrontal cortex and did not extend dorsolaterally into left inferior frontal gyrus (including Brodman area 47), regions commonly engaged in semantic processing of lexical and pictorial material (Thompson-Schill et al., 1997; Poldrack et al., 1999).

The influence of semantic congruency was also examined using a parametric model, which tested for brain

Table 2. Regions Activated by the Interaction of Odors and Pictures

Brain Region	MNI Coordinates (mm) x	y	z	Peak *Z*	p value
Main interaction of olfaction × vision (collapsed across congruency)					
Left rostromedial OFC	−15	39	−15	3.18	$p = 0.059$[a]
Left posterior IPS	−27	−81	18	4.10	$p < 0.001$
Right posterior IPS	33	−69	24	3.18	$p < 0.001$
Left posterior cingulate cortex	−9	−24	36	3.27	$p < 0.001$
Right STS	66	−42	6	3.26	$p < 0.001$
Interaction of olfaction × vision (bimodal congruent condition only)					
Left rostromedial OFC	−15	39	−15	3.42	$p < 0.05$[a]
Left posterior IPS	−36	−78	18	3.82	$p < 0.001$
	−24	−81	21	3.30	$p < 0.001$
Right STS	66	−42	6	3.33	$p < 0.001$
Interaction of olfaction × vision (bimodal incongruent condition only)					
Left posterior cingulate cortex	−9	−24	36	3.62	$p < 0.001$
Left posterior IPS	−24	−81	21	3.42	$p < 0.001$

[a] Corrected for multiple comparisons across a small volume of interest.

activations showing a linear correlation with each subject's own post hoc congruency ratings. In this manner, we eliminated any assumptions about the degree of semantic congruency between odor and picture stimuli. This less-constrained method revealed significant effects in anterior hippocampus (−27, −12, −27; $Z = 4.01$; $p < 0.05$ SVC) and rostromedial OFC (9, 42, −24; $Z = 3.92$; $p < 0.05$ SVC; and −3, 36, −21; $Z = 3.18$; $p < 0.001$ uncorrected), reflecting increased neural responses with subjectively higher ratings of semantic congruency (Figure 6). Of note, these activations closely overlapped the peak responses identified in the primary congruency model (Table 3). In particular, by masking the activations with the contrast of [OV-c] − [OV-i] (thresholded at $p < 0.001$), we confirmed that the parametrically modulated responses observed in hippocampus (−27, −12, −27) and OFC (−3, 36, −21) were within the same regions evident in the main effect of congruency.

Discussion

The aim of this study was to characterize mechanisms underlying visual modulation of olfactory perception. Using a low-level odor detection task, we demonstrated that olfactory detection was faster and more accurate when odors appeared in the context of semantically congruent visual cues (Figure 2). By contrasting congruent and incongruent bimodal conditions, we identified the substrates of this behavioral effect, evident in a congruency-specific activity in anterior hippocampus and rostromedial OFC (Figure 5). Interestingly, while OFC is a consistent target of olfactory activation in human neuroimaging studies (Zatorre et al., 1992; Zald and Pardo, 1997; Yousem et al., 1997), neural responses in hippocampus have been detected less commonly (Small et al., 1997; Sobel et al., 2000; Poellinger et al., 2001). The effects we describe cannot be attributed to differences in stimulus features, since the identities of odors and pictures were matched across congruent and incongruent conditions. Neither can the effects be confounded by odor valence or edibility, since the results were seen over a range of pleasant/unpleasant and food/nonfood odors. Moreover, these findings were observed in the absence of significant differences in sniff patterns. Indeed, the robustness of these activations was particularly evident in a related parametric model, which revealed similar patterns when the subjects' own post hoc congruency ratings were used to model the evoked hemodynamic response (Figure 6).

The behavioral findings show that mere presentation of a visual cue is insufficient to facilitate olfactory perception. Instead, the effect critically relies on access to semantically concordant information, as exemplified in

Table 3. Regions Activated by Semantic Congruency

Brain Region	MNI Coordinates (mm) x	y	z	Peak *Z*	p value
Congruent − incongruent					
Left anterior hippocampus	−27	−12	−24	4.26	$p < 0.05$[a]
Left rostromedial OFC	−3	39	−18	3.72	$p < 0.05$[a]
	−12	42	−18	3.60	$p < 0.05$[a]
Increasing semantic congruency (parametrically modulated by ratings)					
Left anterior hippocampus	−27	−12	−27	4.01	$p < 0.05$[a]
Right rostromedial OFC	9	42	−24	3.92	$p < 0.05$[a]
Left rostromedial OFC	−3	36	−21	3.18	$p < 0.001$

[a] Corrected for multiple comparisons across a small volume of interest.

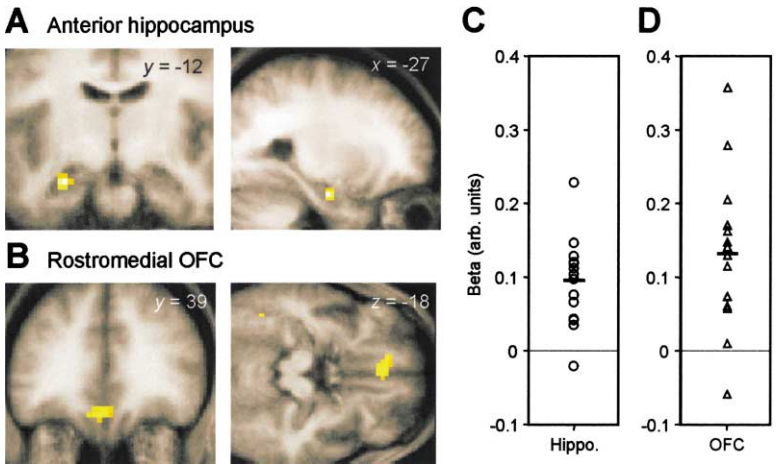

Figure 5. Brain Activations Evoked by Crossmodal Semantic Congruency

(A) Significant areas of activity were seen in left anterior hippocampus. The SPM is overlaid on coronal and sagittal sections of the averaged T1-weighted anatomical scan ($p < 0.001$).

(B) Activations were also observed in rostromedial OFC and are superimposed on coronal and horizontal sections of the T1-weighted image ($p < 0.001$).

(C and D) The beta values derived from the contrast of (OV-c − OV-i) are plotted for each subject in (C) hippocampus and (D) OFC. The mean values are indicated by short horizontal bars.

the congruent versus incongruent distinction. To this end, the congruency-evoked hippocampal responses can be interpreted as mediating retrieval or reactivation of semantic associations between odors and pictures. Existing evidence implicates the hippocampal system in associative or relational processing between multiple sensory information sources (Eichenbaum et al., 1996; Mishkin et al., 1997; Schacter and Wagner, 1999; Brown and Aggleton, 2001). The "binding" together of crossmodal stimuli across disparate brain regions would reflect one such instantiation of this process, a proposal compatible with anatomical considerations of hippocampal organization (Jones and Powell, 1970; Van Hoesen and Pandya, 1975; Mishkin et al., 1997). As the final recipient of converging sensory inputs from entorhinal, perirhinal, and parahippocampal cortices, the hippocampus is especially suited to record and retrieve complex (e.g., crossmodal) associations. We also note that patients with relatively selective hippocampal injury are specifically impaired on tests of associative crossmodal recognition, including face-voice, object-place, and picture-name associations, despite normal (within-modal) item recognition (Vargha-Khadem et al., 1997; Mayes et al., 1999). Moreover, human imaging studies of associative (crossmodal) recognition memory consistently show significant activation in hippocampal areas (Gabrieli et al., 1997; Stark and Squire, 2000; Sperling et al., 2001) similar in location to those described here.

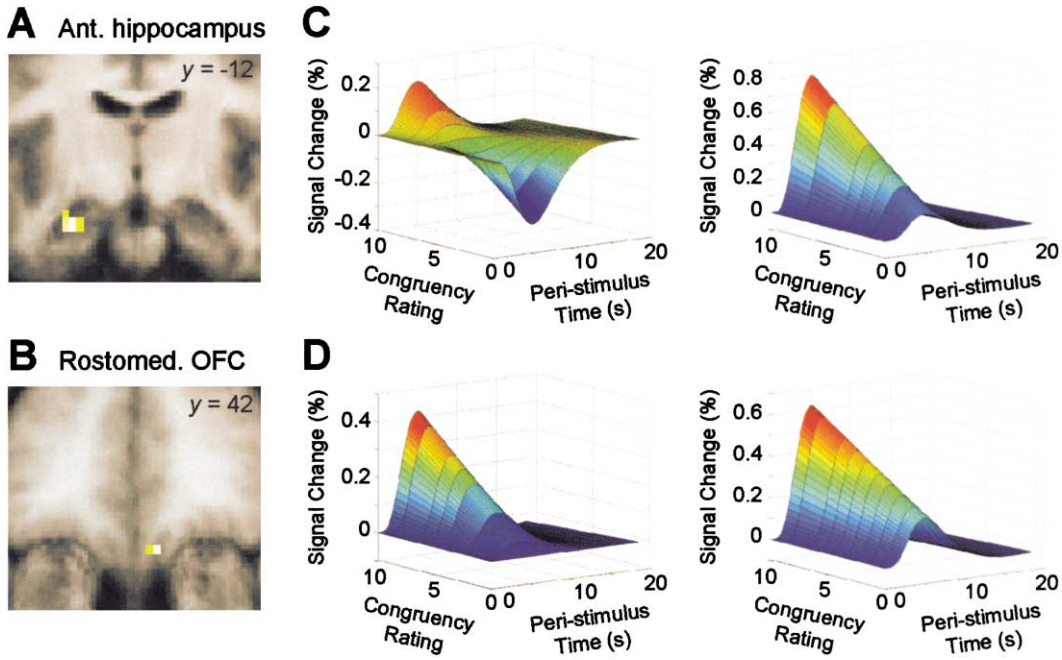

Figure 6. Brain Activations Correlating with Subjective Ratings of Semantic Congruency

(A and B) Neural activations in (A) anterior hippocampus and (B) rostromedial OFC were sensitive to the perceived degree of semantic congruency between odor-picture pairs. The SPMs are shown on coronal sections of the averaged anatomical image ($p < 0.001$).

(C and D) Parametric plots of the data were assembled from four representative subjects and illustrate that the percent (fitted) signal change increased with higher subjective ratings of perceived congruency in (C) hippocampus and (D) OFC.

It is important to reiterate that the correlation between hippocampal activity and perceived semantic congruency occurred during a low-level odor detection task. Specifically, subjects were not asked to make explicit semantic or mnemonic judgments. This implies that hippocampal-mediated reactivation of olfactory-visual semantic associations was obligatory, not requiring the engagement of intentional memory. One question raised by the findings is whether semantic congruency effects could reflect other nonassociative functions, such as detection of semantic novelty (Tulving et al., 1996) or disambiguation of odor events (Levy, 1996). For example, rodent lesion studies show that the hippocampal formation may disambiguate complex odor sequences, particularly when high degrees of interference are present (Agster et al., 2002). Regardless of the actual mechanism, it is evident from numerous imaging studies that both perceptual salience and semantic elaboration, in the absence of overt memory tasks, can engage the anterior hippocampus (Vandenberghe et al., 1996; Dolan and Fletcher, 1997; Martin et al., 1997; Henke et al., 1999; Strange et al., 1999). Our findings extend these principles to the olfactory domain and provide evidence that human hippocampal function is not restricted to intentional memory processes but also supports relatively automatic retrieval of semantic associations.

Within orbitofrontal regions, we observed functionally dissociable patterns of activity that varied with the contrasts of interest. Centroposterior OFC activation in the main effect of olfactory stimulation (Figure 3) closely overlaps OFC areas identified in previous fMRI studies of low-level odor processing (Zatorre et al., 1992; Yousem et al., 1997; Sobel et al., 1998; Gottfried et al., 2002a). This region likely corresponds to secondary olfactory cortex documented in nonhuman primates (Yarita et al., 1980; Carmichael et al., 1994) and may participate in elementary odor computations. In contrast, both the odor × picture interaction (Figure 4) and the direct effect of semantic congruency (Figure 5) activated more medial and rostral OFC zones at least 1.5 cm away from "olfactory" OFC and adjacent to areas engaged in olfactory-visual associative conditioning (Gottfried et al., 2002b). This suggests that by accessing relevant semantic information, rostral OFC may contribute to resolving ambiguity in odor perception and perhaps bias selection of appropriate behavioral strategies, in keeping with its ascribed role in animal models of olfactory learning (Rolls et al., 1996; Gallagher et al., 1999; Schoenbaum et al., 1999). Moreover, the orbitofrontal axis of specialization described here (caudal/rostral) broadly conforms to the topography of primate OFC. In this scheme, unimodal sensory afferents terminating in posterior OFC give rise to projections that converge upon more anteromedial territories (Carmichael and Price, 1996; Ongur and Price, 2000), thereby permitting a synthesis of multimodal information. Our results suggest that similar patterns of regional segregation are preserved in human OFC. In combination with our previous findings regarding olfactory conditioning (Gottfried et al., 2002b), the present data provide evidence that rostromedial OFC supports a wide variety of higher order olfactory computations, including those that sustain olfactory-visual integration.

In the odor × picture interaction, we observed bimodal response enhancements in rostromedial OFC (see above) and posterior IPS (Figure 4). This activation profile may reflect the hemodynamic analog of multisensory integration at the cellular level, as originally demonstrated in cat superior collicular neurons exposed to visual, auditory, and tactile stimuli (Stein and Meredith, 1993). Recently, the phenomenon has been extended to human imaging studies of audio-visual integration (Calvert et al., 2000). Our findings show that this response pattern is applicable to chemosensory modalities in the human brain and imply that heteromodal sites in IPS and STS, long classified in nonolfactory terms, may be tuned to a wider sensory spectrum. Potential roles for olfactory-visual integration in IPS might be to enhance odor source localization or to help orient attention toward a particular odor. While direct olfactory-parietal projections have not been described, the manifestation of olfactory neglect in patients with right parietal lobe damage (Bellas et al., 1988) concurs with the notion that representations of odor space might depend on the function of these regions. Alternatively, we note that activations in posterior parietal cortex and OFC have been elicited in recent PET studies of odor recognition memory (Savic et al., 2000) and working memory (Dade et al., 2001), raising the possibility that, in our study, coincidental olfactory and visual inputs trigger active mnemonic processes. Future studies that focus on more explicit memory tasks will ultimately be required to test this hypothesis.

A central prediction arising from studies of multisensory integration states that measures of performance or behavior should be enhanced, particularly when a stimulus in one modality is ambiguous or underdetermined (Stein and Meredith, 1993). Among the human senses, olfaction may qualify as one of the more indeterminate. Indeed, in the wake of a fleeting odor, trying to decide "What was that smell?" or "Where did that smell come from?" can be insoluble without a relevant sensory, especially visual, cue. We provide behavioral confirmation of this for the visual domain and show that crossmodal facilitation of olfactory perception engages hippocampus and OFC. The dependence of effective olfactory processing on vision goes some way to explain why the perception of smells, even the apparent telltale bouquet of a red Bordeaux, would appear to need the eye of the beholder.

Experimental Procedures

Subjects

Informed consent was obtained from 17 healthy, right-handed subjects (13 women; age range, 22–34 years). Due to poor behavioral performance, 2 subjects (1 woman) were excluded. The experiment was conducted with approval from the joint National Hospital of Neurology and Neurosurgery/Institute of Neurology Ethics Committee.

Stimuli

Olfactory stimuli consisted of four pleasant and four unpleasant odors, comprising a total of eight distinct semantic categories. Two food and two nonfood odors were included within each hedonic class. The pleasant odors were: vanillin (10% w/v in propylene glycol; Sigma-Aldrich, Dorset, UK); sweet orange essential oil (undiluted; Absolute Aromas, Alton, UK); rose maroc essential oil (5% v/v in coconut oil base; Aqua Oleum, Stroud, UK); and pine needle essential oil (50% v/v in mineral oil; Aqua Oleum). The unpleasant

odors were: sour cheese (liquid extract of blue cheese; mixed with 1% v/v 4-methylpentanoic acid, Sigma-Aldrich); rancid fish (mackerel brine; John West, Liverpool, UK; mixed with 0.1% v/v pyridine, Sigma-Aldrich); sulfur smoke (ammonium sulfide, 0.2% v/v in distilled water; Sigma-Aldrich); and paraffin oil (undiluted). Odors were presented using an MRI-compatible, eight-channel computer-controlled olfactometer, capable of rapid delivery of discrete odor pulses in the absence of tactile, thermal, or auditory variation (Gottfried et al., 2002a).

Visual stimuli consisted of 32 high-resolution color images of everyday objects. For each of the eight odors, four different pictures were selected on the basis of shared semantic attributes. For example, pictures of ice cream, cookies, cake, and chocolate were chosen because of their semantic similarity to vanillin odor. When projected into the scanner, the pictures were approximately 4.5 cm wide $\times$ 3 cm high and subtended visual angles of $6^\circ \times 4^\circ$. Both olfactory and visual stimuli were delivered using Cogent 2000 software (Wellcome Dept. of Imaging Neuroscience, London, UK), implemented in Matlab 6.0 (The Mathworks, Inc., Natick, MA).

Task

Subjects participated in an olfactory detection task requiring them to decide whether they smelled an odor or not. The start of each trial ($t = 0$) began with a 1000 ms warning cue (yellow cross-hair), which alerted the subjects to pause their breathing and prepare to sniff (Figure 1A). This was followed by an 850 ms sniff cue (green cross-hair), and subjects sniffed for the duration of the cue. Simultaneously, an odor (unimodal olfactory, "O"), picture (unimodal visual, "V"), both odor and picture (bimodal, "OV"), or neither odor nor picture (low-level baseline, "Bas.") were delivered (Figure 1B). Odor-picture combinations could be semantically congruent ("OV-c") or incongruent ("OV-i"). Note that a sniff was made on every trial, regardless of odor presence. Subjects used a push-button to indicate odor presence ("yes") or absence ("no"), and they were instructed to respond as quickly and as accurately as possible.

Experiment

The experimental paradigm conformed to a modified $2 \times 2 \times 2$ factorial design (Figure 1C). The three within-subject factors were (1) odor (presence/absence); (2) picture (presence/absence); and (3) valence (pleasant/unpleasant). Because the bimodal events were congruent or incongruent, ten different conditions were specified (*pleasant* and *unpleasant* O, V, OV-c, OV-i, Bas.). The baseline (Bas.) events were randomly split into "pleasant" and "unpleasant" categories to maintain orthogonality within the factorial design, but were otherwise identical. The visual stimuli were neutrally valenced, but were designated pleasant and unpleasant, since the pleasant pictures never appeared with unpleasant odors, and vice versa. This ensured that, for a given valence, the only differences between congruent and incongruent conditions were semantic (and not stimulus) attributes.

Trials occurred on average every 8 s ($\pm$1.36 s jitter), for a total of 160 trials (16 trials $\times$ 10 conditions). Along with 32 randomly dispersed "null" events (4 s), the experimental duration was approximately 1400 s. Each odor occurred four times each in the O, OV-c, and OV-i conditions. Each picture occurred once each in the V, OV-c, and OV-i conditions. Thus, 32 unique OV-c events and 32 unique OV-i events were presented during the experiment. Event order was fully randomized, except for the following constraints, in order to minimize the effects of odor habituation and stimulus repetition: (1) per each 1/4 of the experiment, the eight odors occurred only once each in the O, OV-c, and OV-i conditions; and (2) per each 1/4 experiment, the picture presentations were organized such that the eight semantic categories occurred only once each in the V and OV-c conditions.

Behavioral Measurements

Reaction times (RTs) and odor-detection accuracy were measured from all subjects and averaged across each condition type. Respiratory data was also collected on-line from 14 subjects (Gottfried et al., 2002a). A pair of breathing belts (Siemens, Erlangen, Germany) were fastened around the chest and abdomen of each subject and coupled to a differential pressure sensor (0–1 psi; Honeywell, Morristown, NJ). Resulting waveforms were sampled at 100 Hz, recorded on computer using Spike2 software (version 3.16, Cambridge Electronic Design Ltd., Cambridge, UK), and analyzed off-line in Matlab 6.0 (The Mathworks Inc.). Finally, at the completion of the experiment, post hoc ratings of perceived semantic congruency between each odor and the eight paired pictures were obtained (0 = "totally dissimilar"; +10 = "extremely similar") from each subject. Post hoc ratings of odor valence (−10, extremely unpleasant; +10, extremely pleasant) were also collected. Statistical analysis was performed using SPSS for Windows (version 8.0, SPSS Inc., Chicago, IL).

Image Acquisition and Analysis

Gradient echo, T2*-weighted echoplanar images (EPI) with blood-oxygen level-dependent (BOLD) contrast were acquired on a 2T Siemens Vision MRI scanner (Erlangen, Germany), using a combination of image tilting and z-shimming that reduces signal dropout in basal frontal and medial temporal regions (Deichmann and Turner, 2002; Gottfried et al., 2002a). EPI datasets with whole-brain coverage (39 slices; 2.2 mm slice thickness; 1.5 mm gap) were collected continuously every 2.73 s in an oblique orientation 30° to the anterior commissure-posterior commissure line (rostral > caudal), with the following parameters: echo time, 35 ms; field-of-view, 192 mm; in-plane resolution, 3.0 mm. A total of 528 volumes was acquired, minus 5 "dummy" volumes to permit T1 equilibration. Image preprocessing (SPM99; Wellcome Dept., London, UK) included realignment, slice-time correction, spatial normalization, and smoothing with an 8 mm (full-width half-maximum) Gaussian kernel to permit analysis at the group level (Friston et al., 1995a). Anatomical T1-weighted scans (1 mm in-plane resolution) were also collected and coregistered to each subject's mean functional EPI to produce a group-averaged structural image.

The event-related fMRI data was analyzed in SPM99 using the general linear model (Friston et al., 1995b). Ten regressors of interest, corresponding to the onset times for the ten different conditions, were convolved with a canonical hemodynamic response function (HRF) and its temporal derivative. Subject-specific movement parameters and a high-pass filter (cut-off, 120 s) were included. The parameter estimates (betas) for each regressor were calculated for all brain voxels, and relevant contrasts of parameter estimates were computed. The contrast images for all subjects were then entered into a series of one-sample t tests, each constituting an SPM{*T*}. This procedure permitted statistical inference at the population level (random-effects analysis).

We examined three principal contrasts. (1) The main effect of olfaction. This tested for regions preferentially activated by olfactory stimulation and served as an internal quality check that the paradigm could reliably elicit odor-evoked responses in predicted areas. (2) The interaction of olfaction $\times$ vision. This follows from the use of a factorial experimental design and highlights regions showing increased activity in the bimodal condition (OV) that exceeds the mere sum of unimodal inputs (O + V). In estimating the interaction, the low-level baseline condition (Bas.) was subtracted from each of the constituents, which is critical to a fully balanced design. This results in the contrast: (OV − Bas.) − ([O − Bas.] + [V − Bas]). Note this technique is identical to that used by Calvert et al. (2000) in their study of audio-visual crossmodal integration, wherein the interaction was computed by subtracting a "rest" baseline from each condition AV, A, and V: (AV − rest) − ([A − rest] + [V − rest]). We also emphasize that, when rearranged, the term is mathematically identical to (OV − V) − (O − Bas.), the difference between the two simple effects (see Friston et al., 1996). This illustrates the meaning of the interaction in the sense that we are testing for regions that respond to olfactory stimulation in the *presence* of pictures (i.e., OV − V) that is over and above the response in the *absence* of pictures (i.e., O − Bas.). (3) The direct effect of semantic congruency. The contrast of (OV-c − OV-i) was used to reveal areas responsive to shared semantic attributes between odors and pictures.

In a separate parametric model, the effect of subjective congruency was explicitly tested. This resembled the primary model, except that we created "congruency" regressors (one for each valence level) by entering the post hoc congruency ratings for every bimodal odor-picture pair (32 pleasant, 32 unpleasant) as linear parametric modulators of the hemodynamic time series. Thus, the main effect

(+1) of the parametric columns tested for regional activations correlating with subjects' own ratings of semantic congruency. It is important to note that because these ratings were collected at the end of the experiment, their use as correlative regressors may not have completely captured the subjects' "on-line" experiences during the actual task. However, we chose not to obtain congruency ratings during the experiment, in order to keep the task constant across all conditions and maintain a uniform mental set, and also to minimize top-down cognitive mechanisms that can influence human olfactory processing (Zatorre et al., 2000).

Activations are reported that survive a threshold of $p < 0.05$ corrected for multiple comparisons, either across whole-brain volume, where appropriate, or using spheres of 8–10 mm radius to define small volumes of interest (Worsley et al., 1996). These were centered at coordinates derived from previous studies of olfactory (Gottfried et al., 2002a) and semantic (Strange et al., 1999) processing. For descriptive purposes, we report any additional activations in a priori brain regions at $p < 0.001$ uncorrected. Peak maxima are presented in MNI (Montreal Neurological Institute) coordinate space. For the contrasts of principal interest (main effect of olfaction, interaction of olfaction $\times$ vision, congruent minus incongruent), we only considered peak activations that did not show an interaction with valence (at $p < 0.05$ uncorrected), except where specifically indicated. This constraint further controlled Type I error and ensured the primary contrasts were not driven by valence differences.

Acknowledgments

We would like to thank Profs. K. Friston and M. Rugg for constructive comments and advice on data analysis. We also thank P. Bentley, J. Kilner, E. Maguire, B. Strange, and J. Winston for helpful discussions, and the radiographers of the Functional Imaging Laboratory for technical assistance. This work was supported by a Howard Hughes Medical Institute Physician-Postdoctoral Fellowship grant to J.A.G. and a Wellcome Trust Programme grant to R.J.D.

Received: January 22, 2003
Revised: March: 24, 2003
Accepted: June 8, 2003
Published: July 16, 2003

References

Agster, K.L., Fortin, N.J., and Eichenbaum, H. (2002). The hippocampus and disambiguation of overlapping sequences. J. Neurosci. *22*, 5760–5768.

Amaral, D.G., and Price, J.L. (1984). Amygdalo-cortical projections in the monkey (Macaca fascicularis). J. Comp. Neurol. *230*, 465–496.

Andersen, R.A. (1997). Multimodal integration for the representation of space in the posterior parietal cortex. Philos. Trans. R. Soc. Lond. B Biol. Sci. *352*, 1421–1428.

Anderson, A.K., Christoff, K., Stappen, I., Panitz, D., Ghahremani, D.G., Glover, G., Gabrieli, J.D., and Sobel, N. (2003). Dissociated neural representations of intensity and valence in human olfaction. Nat. Neurosci. *6*, 196–202.

Bellas, D.N., Novelly, R.A., Eskenazi, B., and Wasserstein, J. (1988). The nature of unilateral neglect in the olfactory sensory system. Neuropsychologia *26*, 45–52.

Brown, M.W., and Aggleton, J.P. (2001). Recognition memory: what are the roles of the perirhinal cortex and hippocampus? Nat. Rev. Neurosci. *2*, 51–61.

Bruce, C., Desimone, R., and Gross, C.G. (1981). Visual properties of neurons in a polysensory area in superior temporal sulcus of the macaque. J. Neurophysiol. *46*, 369–384.

Bushara, K.O., Grafman, J., and Hallett, M. (2001). Neural correlates of auditory-visual stimulus onset asynchrony detection. J. Neurosci. *21*, 300–304.

Cain, W.S. (1979). To know with the nose: keys to odor identification. Science *203*, 467–470.

Calvert, G.A., Campbell, R., and Brammer, M.J. (2000). Evidence from functional magnetic resonance imaging of crossmodal binding in the human heteromodal cortex. Curr. Biol. *10*, 649–657.

Calvert, G.A., Hansen, P.C., Iversen, S.D., and Brammer, M.J. (2001). Detection of audio-visual integration sites in humans by application of electrophysiological criteria to the BOLD effect. Neuroimage *14*, 427–438.

Carmichael, S.T., and Price, J.L. (1995). Sensory and premotor connections of the orbital and medial prefrontal cortex of macaque monkeys. J. Comp. Neurol. *363*, 642–664.

Carmichael, S.T., and Price, J.L. (1996). Connectional networks within the orbital and medial prefrontal cortex of macaque monkeys. J. Comp. Neurol. *371*, 179–207.

Carmichael, S.T., Clugnet, M.C., and Price, J.L. (1994). Central olfactory connections in the macaque monkey. J. Comp. Neurol. *346*, 403–434.

Cavada, C., and Goldman-Rakic, P.S. (1989). Posterior parietal cortex in rhesus monkey. II. Evidence for segregated corticocortical networks linking sensory and limbic areas with the frontal lobe. J. Comp. Neurol. *287*, 422–445.

Cerf-Ducastel, B., Van de Moortele, P.F., MacLeod, P., Le Bihan, D., and Faurion, A. (2001). Interaction of gustatory and lingual somatosensory perceptions at the cortical level in the human: a functional magnetic resonance imaging study. Chem. Senses *26*, 371–383.

Chapman, C.A., Xu, Y., Haykin, S., and Racine, R.J. (1998). Beta-frequency (15–35 Hz) electroencephalogram activities elicited by toluene and electrical stimulation in the behaving rat. Neuroscience *86*, 1307–1319.

Dade, L.A., Zatorre, R.J., Evans, A.C., and Jones-Gotman, M. (2001). Working memory in another dimension: functional imaging of human olfactory working memory. Neuroimage *14*, 650–660.

Dalton, P. (1996). Odor perception and beliefs about risk. Chem. Senses *21*, 447–458.

Dalton, P., Doolittle, N., Nagata, H., and Breslin, P.A. (2000). The merging of the senses: integration of subthreshold taste and smell. Nat. Neurosci. *3*, 431–432.

Deadwyler, S.A., Foster, T.C., and Hampson, R.E. (1987). Processing of sensory information in the hippocampus. CRC Crit. Rev. Clin. Neurobiol. *2*, 335–355.

Deichmann, R., and Turner, R. (2002). Improvement of local BOLD sensitivities in the presence of susceptibility gradients by using tilted slices. Proc. Int. Soc. Magn. Reson. Med. *10*, 1414.

Distel, H., and Hudson, R. (2001). Judgement of odor intensity is influenced by subjects' knowledge of the odor source. Chem. Senses *26*, 247–251.

Dolan, R.J., and Fletcher, P.C. (1997). Dissociating prefrontal and hippocampal function in episodic memory encoding. Nature *388*, 582–585.

Duhamel, J.R., Colby, C.L., and Goldberg, M.E. (1998). Ventral intraparietal area of the macaque: congruent visual and somatic response properties. J. Neurophysiol. *79*, 126–136.

Eichenbaum, H., Morton, T.H., Potter, H., and Corkin, S. (1983). Selective olfactory deficits in case H.M. Brain *106*, 459–472.

Eichenbaum, H., Schoenbaum, G., Young, B., and Bunsey, M. (1996). Functional organization of the hippocampal memory system. Proc. Natl. Acad. Sci. USA *93*, 13500–13507.

Eskenazi, B., Cain, W.S., Novelly, R.A., and Friend, K.B. (1983). Olfactory functioning in temporal lobectomy patients. Neuropsychologia *21*, 365–374.

Friston, K.J., Ashburner, J., Frith, C.D., Poline, J.-B., Heather, J.D., and Frackowiak, R.S.J. (1995a). Spatial registration and normalization of images. Hum. Brain Mapp. *2*, 165–189.

Friston, K.J., Holmes, A.P., Worsley, K.J., Poline, J.-P., Frith, C.D., and Frackowiak, R.S.J. (1995b). Statistical parametric maps in functional imaging: a general linear approach. Hum. Brain Mapp. *2*, 189–210.

Friston, K.J., Price, C.J., Fletcher, P., Moore, C., Frackowiak, R.S., and Dolan, R.J. (1996). The trouble with cognitive subtraction. Neuroimage *4*, 97–104.

Gabrieli, J.D., Brewer, J.B., Desmond, J.E., and Glover, G.H. (1997). Separate neural bases of two fundamental memory processes in the human medial temporal lobe. Science *276*, 264–266.

Gallagher, M., McMahan, R.W., and Schoenbaum, G. (1999). Orbitofrontal cortex and representation of incentive value in associative learning. J. Neurosci. *19*, 6610–6614.

Gottfried, J.A., Deichmann, R., Winston, J.S., and Dolan, R.J. (2002a). Functional heterogeneity in human olfactory cortex: an event-related functional magnetic resonance imaging study. J. Neurosci. *22*, 10819–10828.

Gottfried, J.A., O'Doherty, J., and Dolan, R.J. (2002b). Appetitive and aversive olfactory learning in humans studied using event-related functional magnetic resonance imaging. J. Neurosci. *22*, 10829–10837.

Grigor, J., Van Toller, S., Behan, J., and Richardson, A. (1999). The effect of odour priming on long latency visual evoked potentials of matching and mismatching objects. Chem. Senses *24*, 137–144.

Henke, K., Weber, B., Kneifel, S., Wieser, H.G., and Buck, A. (1999). Human hippocampus associates information in memory. Proc. Natl. Acad. Sci. USA *96*, 5884–5889.

Hikosaka, K., Iwai, E., Saito, H., and Tanaka, K. (1988). Polysensory properties of neurons in the anterior bank of the caudal superior temporal sulcus of the macaque monkey. J. Neurophysiol. *60*, 1615–1637.

Iwai, E., and Yukie, M. (1987). Amygdalofugal and amygdalopetal connections with modality-specific visual cortical areas in macaques (Macaca fuscata, M. mulatta, and M. fascicularis). J. Comp. Neurol. *261*, 362–387.

Jones, E.G., and Powell, T.P.S. (1970). An anatomical study of converging sensory pathways within the cerebral cortex of the monkey. Brain *93*, 793–820.

Kettenmann, B., Jousmaki, V., Portin, K., Salmelin, R., Kobal, G., and Hari, R. (1996). Odorants activate the human superior temporal sulcus. Neurosci. Lett. *203*, 143–145.

Kreiman, G., Koch, C., and Fried, I. (2000). Category-specific visual responses of single neurons in the human medial temporal lobe. Nat. Neurosci. *3*, 946–953.

Levy, W.B. (1996). A sequence predicting CA3 is a flexible associator that learns and uses context to solve hippocampal-like tasks. Hippocampus *6*, 579–590.

Lorig, T.S., Mayer, T.S., Moore, F.H., and Warrenburg, S. (1993). Visual event related potentials during odour labelling. Chem. Senses *18*, 379–387.

Macaluso, E., Frith, C.D., and Driver, J. (2000). Modulation of human visual cortex by crossmodal spatial attention. Science *289*, 1206–1208.

Martin, A., Wiggs, C.L., and Weisberg, J. (1997). Modulation of human medial temporal lobe activity by form, meaning, and experience. Hippocampus *7*, 587–593.

Mayes, A.R., van Eijk, P.A., Gooding, C.L., Isaac, J.S., and Holdstock, J.S. (1999). What are the functional deficits produced by hippocampal and perirhinal cortex lesions? Behav. Brain Sci. *22*, 460–461.

Mishkin, M., Suzuki, W.A., Gadian, D.G., and Vargha-Khadem, F. (1997). Hierarchical organization of cognitive memory. Philos. Trans. R. Soc. Lond. B Biol. Sci. *352*, 1461–1467.

Mizuno, N., Uemura-Sumi, M., Yasui, Y., Konishi, A., and Matsushima, R. (1982). Direct projections from the extrathalamic forebrain structures to the neocortex in the macaque monkey. Neurosci. Lett. *29*, 13–17.

Morecraft, R.J., Geula, C., and Mesulam, M.M. (1993). Architecture of connectivity within a cingulo-fronto-parietal neurocognitive network for directed attention. Arch. Neurol. *50*, 279–284.

Morrot, G., Brochet, F., and Dubourdieu, D. (2001). The color of odors. Brain Lang. *79*, 309–320.

Ongur, D., and Price, J.L. (2000). The organization of networks within the orbital and medial prefrontal cortex of rats, monkeys and humans. Cereb. Cortex *10*, 206–219.

Poellinger, A., Thomas, R., Lio, P., Lee, A., Makris, N., Rosen, B.R., and Kwong, K.K. (2001). Activation and habituation in olfaction—an fMRI study. Neuroimage *13*, 547–560.

Poldrack, R.A., Wagner, A.D., Prull, M.W., Desmond, J.E., Glover, G.H., and Gabrieli, J.D. (1999). Functional specialization for semantic and phonological processing in the left inferior prefrontal cortex. Neuroimage *10*, 15–35.

Rockland, K.S., and Van Hoesen, G.W. (1999). Some temporal and parietal cortical connections converge in CA1 of the primate hippocampus. Cereb. Cortex *9*, 232–237.

Rolls, E.T., and Baylis, L.L. (1994). Gustatory, olfactory, and visual convergence within the primate orbitofrontal cortex. J. Neurosci. *14*, 5437–5452.

Rolls, E.T., Critchley, H.D., Mason, R., and Wakeman, E.A. (1996). Orbitofrontal cortex neurons: role in olfactory and visual association learning. J. Neurophysiol. *75*, 1970–1981.

Royet, J.P., Zald, D., Versace, R., Costes, N., Lavenne, F., Koenig, O., and Gervais, R. (2000). Emotional responses to pleasant and unpleasant olfactory, visual, and auditory stimuli: a positron emission tomography study. J. Neurosci. *20*, 7752–7759.

Sarfarazi, M., Cave, B., Richardson, A., Behan, J., and Sedgwick, E.M. (1999). Visual event related potentials modulated by contextually relevant and irrelevant olfactory primes. Chem. Senses *24*, 145–154.

Save, E., Nerad, L., and Poucet, B. (2000). Contribution of multiple sensory information to place field stability in hippocampal place cells. Hippocampus *10*, 64–76.

Savic, I., Gulyas, B., Larsson, M., and Roland, P. (2000). Olfactory functions are mediated by parallel and hierarchical processing. Neuron *26*, 735–745.

Schacter, D.L., and Wagner, A.D. (1999). Medial temporal lobe activations in fMRI and PET studies of episodic encoding and retrieval. Hippocampus *9*, 7–24.

Schoenbaum, G., Chiba, A.A., and Gallagher, M. (1999). Neural encoding in orbitofrontal cortex and basolateral amygdala during olfactory discrimination learning. J. Neurosci. *19*, 1876–1884.

Schwerdtfeger, W.K., Buhl, E.H., and Germroth, P. (1990). Disynaptic olfactory input to the hippocampus mediated by stellate cells in the entorhinal cortex. J. Comp. Neurol. *292*, 163–177.

Small, S.A. (2002). The longitudinal axis of the hippocampal formation: its anatomy, circuitry, and role in cognitive function. Rev. Neurosci. *13*, 183–194.

Small, D.M., Jones-Gotman, M., Zatorre, R.J., Petrides, M., and Evans, A.C. (1997). Flavor processing: more than the sum of its parts. Neuroreport *8*, 3913–3917.

Sobel, N., Prabhakaran, V., Desmond, J.E., Glover, G.H., Goode, R.L., Sullivan, E.V., and Gabrieli, J.D. (1998). Sniffing and smelling: separate subsystems in the human olfactory cortex. Nature *392*, 282–286.

Sobel, N., Prabhakaran, V., Zhao, Z., Desmond, J.E., Glover, G.H., Sullivan, E.V., and Gabrieli, J.D. (2000). Time course of odorant-induced activation in the human primary olfactory cortex. J. Neurophysiol. *83*, 537–551.

Sperling, R.A., Bates, J.F., Cocchiarella, A.J., Schacter, D.L., Rosen, B.R., and Albert, M.S. (2001). Encoding novel face-name associations: a functional MRI study. Hum. Brain Mapp. *14*, 129–139.

Stark, C.E., and Squire, L.R. (2000). fMRI activity in the medial temporal lobe during recognition memory as a function of study-test interval. Hippocampus *10*, 329–337.

Stein, B.E., and Meredith, M.A. (1993). The Merging of the Senses (Cambridge, MA: The MIT Press).

Strange, B.A., Fletcher, P.C., Henson, R.N., Friston, K.J., and Dolan, R.J. (1999). Segregating the functions of human hippocampus. Proc. Natl. Acad. Sci. USA *96*, 4034–4039.

Suzuki, W.A., and Amaral, D.G. (1994). Perirhinal and parahippocampal cortices of the macaque monkey: cortical afferents. J. Comp. Neurol. *350*, 497–533.

Thompson-Schill, S.L., D'Esposito, M., Aguirre, G.K., and Farah, M.J. (1997). Role of left inferior prefrontal cortex in retrieval of semantic

knowledge: a reevaluation. Proc. Natl. Acad. Sci. USA *94*, 14792–14797.

Tulving, E., Markowitsch, H.J., Craik, F.E., Habib, R., and Houle, S. (1996). Novelty and familiarity activations in PET studies of memory encoding and retrieval. Cereb. Cortex *6*, 71–79.

Van Hoesen, G.W., and Pandya, D.N. (1975). Some connections of the entorhinal (area 28) and perirhinal (area 35) cortices of the rhesus monkey. III. Efferent connections. Brain Res. *95*, 39–59.

Vandenberghe, R., Price, C., Wise, R., Josephs, O., and Frackowiak, R.S. (1996). Functional anatomy of a common semantic system for words and pictures. Nature *383*, 254–256.

Vanderwolf, C.H. (2001). The hippocampus as an olfacto-motor mechanism: were the classical anatomists right after all? Behav. Brain Res. *127*, 25–47.

Vargha-Khadem, F., Gadian, D.G., Watkins, K.E., Connelly, A., Van Paesschen, W., and Mishkin, M. (1997). Differential effects of early hippocampal pathology on episodic and semantic memory. Science *277*, 376–380.

Wood, E.R., Dudchenko, P.A., and Eichenbaum, H. (1999). The global record of memory in hippocampal neuronal activity. Nature *397*, 613–616.

Worsley, K.J., Marrett, S., Neelin, P., Vandal, A.C., Friston, K.J., and Evans, A.C. (1996). A unified statistical approach for determining significant voxels in images of cerebral activation. Hum. Brain Mapp. *4*, 58–73.

Yarita, H., Iino, M., Tanabe, T., Kogure, S., and Takagi, S.F. (1980). A transthalamic olfactory pathway to orbitofrontal cortex in the monkey. J. Neurophysiol. *43*, 69–85.

Yousem, D.M., Williams, S.C., Howard, R.O., Andrew, C., Simmons, A., Allin, M., Geckle, R.J., Suskind, D., Bullmore, E.T., Brammer, M.J., and Doty, R.L. (1997). Functional MR imaging during odor stimulation: preliminary data. Radiology *204*, 833–838.

Zald, D.H., and Pardo, J.V. (1997). Emotion, olfaction, and the human amygdala: amygdala activation during aversive olfactory stimulation. Proc. Natl. Acad. Sci. USA *94*, 4119–4124.

Zatorre, R.J., Jones-Gotman, M., Evans, A.C., and Meyer, E. (1992). Functional localization and lateralization of human olfactory cortex. Nature *360*, 339–340.

Zatorre, R.J., Jones-Gotman, M., and Rouby, C. (2000). Neural mechanisms involved in odor pleasantness and intensity judgments. Neuroreport *11*, 2711–2716.

Zellner, D.A., and Kautz, M.A. (1990). Color affects perceived odor intensity. J. Exp. Psychol. Hum. Percept. Perform. *16*, 391–397.